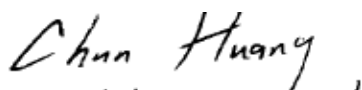**Surface Hydrophilization of Polysulfone Membrane by Cyclonic Atmospheric Pressure Plasma**

Ching-Yuan Tsai, Ya-Chi Chang, and Chun Huang [*]

Department of Chemical Engineering & Materials Science, Yuan Ze University, 135 Yuan-Tung

Road, Chung-Li, 32003, Taiwan.

Chun Huang

_____

[*]E-mail address: chunhuang@saturn.yzu.edu.tw

I am the corresponding author and my address and other information is as follows:

Tel: 886- 03-463-8800 ext. 3551
Fax: 886- 03- 4559373
E-mail: chunhuang@saturn.yzu.edu.tw
Address: 135 Yuan-Tung Road, Chung-Li, 32003, Taiwan.

Surface Hydrophilization of Polysulfone Membrane by Cyclonic Atmospheric Pressure Plasma

Ching-Yuan Tsai, Ya-Chi Chang and Chun Huang [*]

Department of Chemical Engineering & Materials Science, Yuan Ze University, 135 Yuan-Tung Road, Chung-Li, Taiwan 32003.

Abstract

Atmospheric-pressure plasma treatments in a 13.56 MHz radio frequency (RF) glow discharge were employed to modify the polysulfone (PSF) membrane surfaces to improve the hydrophilicity and surface modification. The change of hydrophilicity was monitored by static contact angle measurement. The polysulfone membrane surfaces became highly hydrophilic when exposed for only 15 sec to the cyclonic atmospheric-pressure plasma. A significant increase in the surface energy of polysulfone membranes due to CASING effect was observed. Optical emission spectroscopy (OES) was employed to investigate the various chemical species of cyclonic atmospheric-plasma processing. Chemical structure and surface morphological changes on the membrane surface were characterized by X-ray photoelectron spectroscopy (XPS) and field emission scanning electron microscopy (FESEM). XPS analysis showed significantly higher surface concentrations of oxygen functional groups for cyclonic atmospheric-pressure plasma-activated PSF membrane surfaces than originally unmodified PSF membrane surfaces. The experimental results reveal that cyclonic atmospheric-pressure plasma processing is an effective method to improve the surface hydrophilicity of PSF membranes.

Keywords: polysulfone membrane, surface characteristics, cyclonic atmospheric plasma, CASING effect, polysulfone membrane

1. Introduction

As a promising technique in plasma technology, atmospheric-pressure plasma has attracted numerous attentions from both academic and industrial researchers and is being actively investigated for a variety of applications including in film deposition, surface cleaning, etching, surface modification, sterilization, pollution control, etc [1-4]. In atmospheric-pressure plasma technique, plasma surface modification on polymers is an active research field since the society greatly demands an effective, efficient and simple surface modification method for a wide range of polymers. To date, most of the research efforts in atmospheric-pressure plasma have been focusing on increasing plasma dimension or extending discharge gap between the electrodes in order to make the plasma sources more suitable to large scale surface modification [4-10]. Many of the investigations have been devoted to elucidate the atmospheric-pressure plasma surface modification on polymeric materials in order to optimize the modification processes and thus improve its efficiency [11-13]. However, despite the extensive studies of atmospheric-pressure plasma surface modification on non-porous polymeric materials, the surface activation of porous polymeric materials such as membranes by atmospheric-pressure plasma has not been extensively examined and reported.

Polysulfone (PSF) is a commercially available, thermoplastic polymer used in separation processes due to its mechanical stability, thermal resistance, and excellent film forming properties [14,15]. One issue with PSF membrane is its hydrophobicity. It leads to severe fouling in protein-based ultrafiltration. It extremely resists the long-term use of the PSF membranes in many filtration systems. A useful strategy to avoid the membrane fouling is to improve the membrane surface hydrophilicity by surface modification method [16-18]. In addition, hydrophilic membrane surfaces usually obtain the larger permeation fluxes and the higher reproducility than hydrophobic ones [18,19]. Nanoporous membranes have been widely used for numerous ultrafiltration (UF) processes [20-22].

In the present work ultrafiltration (UF) polysulfone (PSF) membranes were modified by cyclonic atmospheric-pressure plasma with various operational parameters, with the objective of improving the intrinsic low surface properties. The change in hydrophilicity of cyclonic atmospheric-pressure plasma-modified PSF membranes was characterized by measuring the static contact angle method (CA). Optical emission spectroscopy (OES) was used to investigate the various chemical species to cause plasma surface modification. The surface morphology of the cyclonic atmospheric-pressure plasma-treated PSF membranes was analyzed using field emission scanning electron microscopy (FESEM). The chemical composition change of the cyclonic

atmospheric-pressure plasma-modified PSF membrane surfaces were characterized by X-ray photoelectron spectroscopy (XPS). This work is the first step in exploring the potential of cyclonic atmospheric-pressure plasma modification as a mean of improving the surface hydrophilicity of ultrafiltration (UF) polysulfone (PSF) membranes.

2.   Experimental Details

2.1. Atmospheric pressure plasma deposition system

Polysulfone (PSF) membranes were modified by cyclonic atmospheric-pressure plasma system as shown in Figure 1(a). The novel design of this atmospheric-pressure plasma is based on the use of two rotating double-pipe type discharge jets to form plasma cyclone at a plasma rotational speed of at least 440 rpm. The cyclonic atmospheric-pressure plasma consists of a gas compartment and two discharge jets placed certain distance apart inside the gas compartment. The double-pipe type discharge jets used for the cyclonic atmospheric-pressure plasma treatment are similar to that reported in [2]. The high-speed gas flow rate argon (10 slm) is introduced from the upside the plasma system and passes through the gas compartment as the ionization gas. An electrical field is applied to ignite the plasma glow discharge by a 13.56 MHz radio frequency (RF) power supply. A capacitive coupled RF plasma source power is in continuous mode. The sample is mounted on an X-Y movable table in order to simulate in-line processing at variable line speeds. Because of this movement, the plasma volume increases dramatically from the thin cyclone discharge thread without the crossed fields to a large region. Figure 1(b) shows the infrared thermal imaging of cyclonic atmospheric-pressure plasma with touching the substrate. The sensitivity of infrared thermal measuring technique is 150 mk at 25℃ scene temperature. The radiant temperature profile of cyclonic atmospheric-pressure plasma measured by infrared thermal analysis was similar to those by thermocouple thermometer analysis in Figure 1(b) at low temperature (30 ℃ - 85 ℃) measured with a thermocouple thermometer.

2.2. Modified surface characterization and analysis

Argon gas which used to create atmospheric-pressure plasma was an industrial grade with 99.995% purity and purchased from Min-Yang Gas Corporation. Polysulfone (PSF) membrane samples (0.1 mm thick) were supplied by R&D Center for Membrane Technology, Chung Yuan University, Chungli, Taiwan. The PSF membranes were cut into strips and were used as samples for atmospheric-pressure plasma surface modification experiments. Prior to use in experiment, each polysulfone membrane samples was cleansed in an ultrasonic soap water bath for 20 minutes, thoroughly rinsed with DI water for 30 minutes, and dried completely in the air. The static contact

angles of polysulfone membrane samples were measured by projecting an image of an automatic sessile droplet resting on a membrane surface with a Magic Droplet Model 100SB Video Contact Angle System (Sindatek Instruments Corporation, Taipei, Taiwan). After the atmospheric-pressure plasma modification treatments, the untreated PSF membrane samples and the plasma modified PSF membrane samples were placed on a vertically and horizontally adjustable sample stage. After the 0.1 µL water droplet has made contact with the polymer surface, a snapshot of the image was taken. The captured image was saved and contact angle measurements were commenced at leisure. In order to understand the nature of the surface change of PSF membranes, the dispersion and polar interaction contributions to the surface energy of the materials were calculated using the Owens–Wendt model [23]. The liquids used for calculating the surface energies of the untreated and plasma-treated PP membranes were water and di-iodomethane of known γ^p (polar component) and γ^d (disperse component). The surface energy of a solid (γ^s) has two components, namely, a polar component and a disperse component. Both components contribute to the total surface energy. The polar and disperse components are responsible for the hydrophilic and hydrophobic properties, respectively.

The major plasma diagnostic apparatus of atmospheric-pressure plasma is an optical emission spectroscopy. This equipment consists of both the instrumentation and spectrum analysis software, which was supplied by Hong-Ming Technology, Inc. The observable spectral range was 250-950 nm with a resolution of 2 nm. The surface morphology of the plasma treated polysulfone membranes were examined by field emission scanning electron microscopy (FESEM), respectively. FESEM analysis was performed with a JEOL model JSM-6701f scanning electron spectroscopy apparatus at Department of Chemical Engineering & Materials Science, Yuan Ze University. Au coatings 20 nm thick was evaporated onto the polysulfone membrane surface (1x1 cm^2) to get a conducting surface. A tungsten filament was used as the electron source. A 5-KeV accelerator voltage was used for scanning the sample surfaces. A VG Scientific Microlab 310F system equipped with Mg Kα X-ray source (1253.6 eV) and a concentric hemispherical analyzer was used for X-ray photoelectron spectroscopy (XPS) surface analysis. Spectra were acquired with the angle between the direction of the emitted photoelectrons and the surface of polysulfone membranes equal to take-off analysis angle 70°. For the evaluation of the differences in the porosity caused by the usage of cyclonic atmospheric-pressure plasma, the porosity of the untreated PSF membrane samples and the plasma modified PSF membrane samples were studied. The size distribution of the pores of PSF membrane samples was calculated from a N_2 sorption isotherm (ASAP 2020, Micromeritics).

3. Results and discussion

Optical emission spectroscopy was used to detect the excited plasma reactive species generated

by cyclonic atmospheric-pressure plasma. The optical emission analysis is expected to explicate the reactions of plasma reactive species that may contribute to polysulfone (PSF) membrane surface modification. The optical emission spectrum of cyclonic atmospheric-pressure plasma is presented in Figure 2. From optical emission spectrum of cyclonic atmospheric-pressure plasma, the strong argon emission lines are dominant at about 700-800 nm. Regarding the strong Ar plasma species from OES analysis, the CASING (Crosslinking via Activated Species of Inert Gases) effect can be recognized as the possible major reason of cyclonic atmospheric-pressure plasma surface modification on PSF membrane. The possible mechanism of generating active sites is due to the radicals released from cyclonic atmospheric-pressure plasma; then, these radicals interact with the PSF membrane surface to generate dangling bonds which then lead to the formation of the surface active sites [12,13]. The obvious emission line of the molecular nitrogen bands between 300-400 nm are also observed in the spectrum, as well as the emission line of the oxygen atom at 777 nm and 844 nm from the ambient air. The low intensity of emission derived from OH band system (308.9 nm) was observed as well. It is supported the assumption that atmospheric-pressure plasma surface modification as a result of the electron-impact-dissociation of ambient air [12]. From optical emission analysis of cyclonic atmospheric-pressure plasma, it indicates corresponds to the possible surface modification effect of Ar, N, and O plasma species. In addition, the plasma surface modification can be also attributed to the interaction of oxygen-based plasma species in the atmospheric-pressure plasma with polymers [24]. The oxygen-based plasma species such as O and O_3 radicals can create oxygen-containing groups through oxidation processes.

Static contact angle measurement is one of the simplest methods used for the examination of surface property changes that appear on PSF membrane surface after a plasma surface modification. We used this method to evaluate surface energy of cyclonic atmospheric-pressure plasma-modified PSF membranes. The effect of plasma treatment time on surface energy, and both its contact angles, is shown in Figure 3, respectively. In improving the hydrophilicity of PSF membrane, the longer plasma treatment time was more capable than the shorter plasma treatment time. Figure 3 also shows a plot of surface energy (γ^s) from the measured static contact angle values on the cyclonic atmospheric-pressure plasma-modified PSF membrane surfaces as a function of treatment time. The surface energy of the unmodified PSF membrane is 51 mJ/m^2. The changes in the surface energy of cyclonic atmospheric-pressure plasma-modified PSF membrane surfaces notably increased after a very short treatment time (15 sec.). These results show that the cyclonic atmospheric-pressure plasma is efficient in the hydrophilicity modification of the membrane surface. Table 1 summarized the static contact angle values of two suitable liquids (D.I water and di-iodomethane) and surface free energies of untreated and cyclonic atmospheric-pressure plasma-modified PSF membrane surfaces. This result confirmed that the plasma treatment made the porous polymeric material

surface more hydrophilic at a certain level depending on the operational conditions.

Figure 4 shows the static contact angle and surface energy changes of cyclonic atmospheric-pressure plasma-modified PSF membranes with argon gas flow rate of the plasma under a fixed radio frequency (RF) power and plasma treatment time. As shown in Figure 4, the static contact angle values of atmospheric-pressure plasma-modified PSF membranes gradually decreased with increasing argon gas flow rate. The increase in the argon gas flow rate could lead to an increase in the surface concentration of polar functional groups on the PSF membrane. This can be demonstrated by the fact that the polar contribution gradually increases with respect to the increase in the reactive plasma species. It is believed that reactive species in the plasma gas phase, which can react with the activated surface, become abundant with increasing argon gas flow. Therefore, the number of activated sites on the surface is lower than with low argon gas flow rate only.

Figure 5 shows the contact angle and surface energy changes of cyclonic atmospheric-pressure plasma-modified PSF membranes with various RF plasma power levels. The changes in the contact angle change of cyclonic atmospheric-pressure plasma-modified PSF membrane significantly increased with rising RF plasma power. The most efficient RF plasma power level was 150 watt, where an effective surface modification was achieved on polysulfone membrane with low plasma power consumption. In addition, the increasing RF plasma power level in Figure 5, produced a significant surface modification effect in lowering the water contact angles on the PSF membrane surface. As can be seen from Figure 5, 150 watt of plasma power level significantly improved the surface energy of the PSF membrane from 51 mJ/m^2 to 77 mJ/m^2. It is clear from Figure 5 that the surface property of polysulfone membrane is significantly increased and becomes hydrophilic by cyclonic atmospheric-pressure plasma treatments.

In atmospheric-pressure plasmas, the plasma species could lose its reactivity in the short time because of the much higher collision frequency among the plasma particles. The life time of the reactive plasma species is much shorter when compared to that in low-pressure plasmas. As a result, the plasmas could significantly lose their reactivity in a remote position (away from the glow). To study the surface modification effects of plasma afterglow region, PSF membranes were subjected to cyclonic atmospheric-pressure plasma exposure in the down stream at a position 20 mm away from the glow. The long-life plasma species from the plasmas were allowed to diffuse and get in contact with PSF membranes. Figure 6 shows the surface modification effect dependence on a remote plasma exposure and direct plasma exposure. It was observed that the remote plasma exposure causes much slower surface modification influence on cyclonic atmospheric-pressure plasma-modified PSF membranes than the direct plasma exposure from contact angle and surface

free energy data in Figure 6. In Figure 7, the emission intensity change of several Ar and O emission lines was plotted against different vertical positions away from cyclonic atmospheric-pressure plasma. It can be seen that, upon the increasing distance away from the glow region of cyclonic atmospheric-pressure plasma, all major emission lines were quenched and showed the same decreasing tendency with increasing distance. This can be understood due to the fast consumption of reactive plasma species at relatively distant down-stream region. As discussed above, it can be concluded that, under the present operation conditions, the short lifetime of reactive plasma species are primarily responsible for the decreasing modification influence in the afterglow cyclonic atmospheric-pressure plasma.

In general, the surface property treated by plasma surface activation/modification greatly relies on the chemical composition and surface morphology. Besides the possible etching/bombardment of plasma surface activation/modification sensitively affects the change in the surface morphology and roughness [12,17]. To ascertain whether the plasma adversely altered the physical properties (i.e. pore size) of the membrane, FESEM images were obtained for unmodified and cyclonic atmospheric-pressure plasma-modified PSF membranes (Figure 8). Unmodified PSF membrane surface (Figure 8a) is smooth with many round features. Presence of plasma species in cyclonic atmospheric-pressure plasma turns it to more active one-size change of surface porosity are seen already after 60 sec of treatment (Figure 8b). Exposing the samples to plasma action for a longer time causes the extended pore sizes of membrane surface (Figure 8c). These images are compared to that of an unmodified membrane (Figure 8a). It is evident that prolonged exposure to cyclonic atmospheric-pressure plasma introduces visible morphology change of the membrane surface, thereby increasing the porosity of the membrane (Figure 8c).

Static contact angle measurement showed that hydrophilic characteristics were introduced on the membrane surface by cyclonic atmospheric-pressure plasma surface modification. To verify these findings and to supplement them, X-ray photoelectron spectroscopy (XPS) analysis was used to correlate the results obtained by static contact angle measurement, which suggested a significant activation/oxidation at the surface of the cyclonic atmospheric-pressure plasma-modified PSF membranes. A quantitative evaluation of the changes in the atomic concentration in the PSF membrane surfaces as a function of plasma treatment time is summarized in Table 2a. The quantitative data confirm that, the oxygen contents increase and the carbon content decreases. It shows that the ratio of O_{1s}/C_{1s} has increased after cyclonic atmospheric-pressure plasma surface modification. This could be attributed to the increase in the newly formed functional groups by the cyclonic atmospheric-pressure plasma treatment, as will be discussed from the XPS spectra of unmodified and cyclonic atmospheric-pressure plasma-modified PSF membranes. The XPS survey scans for investigated samples are shown in Figure 9. The enrichment of surface with

7

oxygen-containing functionalities is evident. It would suggest that more free radicals are formed during cyclonic atmospheric-pressure plasma treatment which after exposing to the air takes part in post-reactions.

In order to study the major functional groups introduced into PSF membrane surfaces by cyclonic atmospheric-pressure plasma surface modification, XPS deconvolution analysis of C_{1s} peaks was performed. To show the existence of various forms of carbon, the narrow scans of the region of C_{1s} was analyzed (Figure 9). The partition of carbon to different structures is shown in Table 2b.As shown in Figure 9a, the C_{1s} spectrum of untreated PSF membrane contained two five-separated peaks at 284.7 eV, 285.3 eV, 286.0 eV, 287.1 eV, and 291.7 eV corresponding to C–C/C–H, C-S, C–O, C=O, and π-π* groups, respectively [14,15,24-26]. The spectra of cyclonic atmospheric-pressure plasma-modified PSF membranes with different treatment time (Figure 9b and 9c) also showed these five peaks, at the same time, an additional peak at 290.3 eV also appear and rise which could be attributable to O-C=O groups [15,24].The modifcaiton of cyclonic atmospheric-pressure plasma to the surface can cause an additional increase of 286.0 eV peak for C–O bonds are also detected in this region. As a result of plasma treatment, the CH percentage decreases relative to the untreated PSF membrane. This decrease is counterbalanced by an increase in the percentages of C–O and O-C=O groups. These results suggested that cyclonic atmospheric-pressure plasma treatment cleave the C–C/C–H bonds and introduce oxygen-containing functional groups into the molecular chain of PSF membrane surface [15,24]. These polar groups contribute to increase in the surface hydrophilicity of the PSF membranes. The percentage contribution of the C_{1s} components of cyclonic atmospheric-pressure plasma-modified PSF membranes, calculated from the C_{1s} spectra, is shown in Table 2b. This conclusion is in strong agreement with static contact angle analysis. It was shown that cyclonic atmospheric-pressure plasma could cause creating of new functional groups onto the polymer surface.

Figure 10 shows the presence of two kinds of oxygen in the unmodified PSF membrane; they come from O=S=O (531.8 eV) and O*-C=O (533.1 eV) structures (The XPS analysis of O_{1s} peaks). The new peak could be seen at 532.4 eV (C=O* bond) of cyclonic atmospheric-pressure plasma-treated PSF membranes in Figure 10 and Table 2c. It suggests that the amount of reactive species increases with increasing plasma treatment time, and the activated species can easily form reactive oxygen-containing functional groups on the membrane surface. The activation of the surface and the chemical etching process can occur simultaneously using these reactive species. However, in contrast to the chemical etching process, the modifcaiton of the surface becomes the dominant process with increasing plasma treatment time. For this reason, the more O*-C=O groups

corresponding to higher binding energy remains on the surface in Table 2c because of a minor plasma etching effect.

Plasma surface modification can essentially change the structure of porous membrane-pore size and their distribution. For this reason, to determine the membrane pore size distribution seems to be important in understanding the interaction of membrane and plasma surface modification. In the case of cyclonic atmospheric-pressure plasma treatment of PSF membranes, the method allows also to control the membrane structure. In addition to FESEM analysis, changes in the pore diameter of cyclonic atmospheric-pressure plasma modified PSF membranes were quantified by size distribution of the pores of PSF membrane samples was calculated from a N_2 sorption isotherm (ASAP 2020, Micromeritics). Pore size distribution functions, calculated for the membranes under investigation, are shown in Figure 11. From FESEM detection, the cyclonic atmospheric-pressure plasma surface modification causes a significant increase of pore diameter and widening of size distribution in Figure 8. Pore size distributions of unmodified and 60 sec modified membrane exhibited the significant difference in Figure 11. Overall, the pore sizes are around 25% larger than the pore sizes of unmodified PSF membrane.

4. Conclusion

This investigation demonstrated the efficient surface modification technique of cyclonic atmospheric-pressure plasma. Static contact angle measurement results indicated that this atmospheric-pressure plasma rapidly improves the hydrophilicity and surface energy of nano-porous polysulfone (PSF) membranes. Optical emission spectroscopy determined plasma reactive species from cyclonic atmospheric-pressure plasma which contribute surface modification/activation of PSF membranes. The interaction of reactive plasma species in the plasma with PSF membrane surface can be recognized as the enhancement of surface modification from OES analysis. The polar functional groups generated due to plasma treatment on the surface of PSF membranes causes decrease in contact angle and rise in surface energy. The XPS results showed that the carbon content decreased and the oxygen content increased on the surface of the cyclonic atmospheric-pressure plasma treated PSF membranes. The chemical and surface morphological changes made on surface of PSF membranes lead to increase in hydrophilic properties. The plasma modification capability demonstrated through this study indicated the tremendous potential of this cyclonic atmospheric-pressure plasma as a promising membrane surface modification/activation technique.

References

[1] V. Hopfe, D. W. Sheel, IEEE Trans. Plasma Sci. 35 (2007) 204.

[2] C. Huang, W.T. Hsu, C.H. Liu, S.Y. Wu, S.H. Yang, T.H. Chen, and T.C. Wei, IEEE Trans. Plasma Sci. 37 (2009) 1127.

[3] M. Moravej, R.F. Hicks, Chem. Vapor Deposition 11 (2005) 469.

[4] A. Schütze, J.Y. Jeong, S.E. Babayan, J. Park, G.S. Selwyn, R.F. Hicks, IEEE Trans. Plasma Sci., 26 (1998) 1685-1694.

[5] Y. Duan, C. Huang, Q.S. Yu, IEEE Trans. Plasma Sci. 33 (2005) 328.

[6] Q.S. Yu, C. Huang, F.H. Hsieh, H. Huff, Y. Duan, J. Biomed. Mater. Res. 80 (2007) 211.

[8] Y. Duan, C. Huang, Q.S. Yu, Rev. Sci. Instrum. 78 (2007) 015104.

[9] C. Huang, C.H. Liu, S.Y. Wu, Surf. Interface Anal. 41 (2009) 44.

[10] C. Huang, C.H. Liu, S.Y. Wu, T.H. Chen, J.T. Teng, C.H. Su, C.M. Chen, IEEE Trans. Plasma Sci. 37 (2009) 1169.

[11] H. Yoshiki, A. Oki, H. Ogawa, Y. Horiike, Thin Solid Films 407 (2002) 156

[12] C. Huang, S.Y. Wu, Y.C. Liu, C.Y. Chang, C.Y. Tsai, Jpn. J. Appl. Phys. 50 (2011) 01AH05

[13] C. Huang, C.Y. Chang, S.Y. Wu, Thin Solid Films 518 (2010) 5537

[14] K.S. Kim, K.H. Lee, K. Cho, C.E. Park, J. Membr. Sci. 199 (2002) 135.

[15] D.S. Wavhal, E.R. Fisher, Desalination 172 (2005) 189.

[16] M.L. Steen, L. Hymas, E.D. Havey, N.E. Capps, D.G. Castner, E.R. Fisher, J. Membr. Sci. 188 (2001) 97.

[17] C. Huang, C.Y. Tsai, R.S. Juang, H.C. Kao, J. Appl. Polym. Sci. 118 (2010) 3227.

[18] M.L. Steen, A.C. Jordan , E.R. Fisher, J. Membr. Sci. 204 (2002) 341.

[19] G. Yan, L.Q. Liu, Z.Q. Tang, L. Huang, W. Li, J. Zhou, J.S. Gu, X.W. Wei, H.Y. Yu, Chem. Eng. J. 145(2008) 218.

[20] T.D. Tran, S. Mori, M. Suzuki, Thin Solid Films 515 (2007) 4148

[21] H.Y. Yu, X.C. He, L.Q. Liu, J.S. Gu, X.W. Wei, Water. Res., 41 (2007) 4703.

[22] Y.F. Yang, L.S. Wan, Z.K. Xu, J. Membr. Sci. 337 (2009) 70

[23] D.K. Owens, R.C. Wendt, J. Appl. Polym. Sci. 13 (1969) 1741.

[24] E. Gonzalez, M.D. Barankin, P.C. Guschl, R.F. Hicks, IEEE Trans. Plasma Sci. 37 (2009) 823.

[25] Y.Q. Song, J. Sheng, M. Wei, X.B. Yuan, J. Appl. Polym. Sci. 78 (2000) 979.

[26] J. Qiu, Y. Zhang, Y. Shen, Y. Zhang, H. Zhang, J. Liu, Appl. Surf. Sci. 256 (2010) 3274.

Figure captions

Fig. 1 (a) Schematic diagram of cyclonic atmospheric-pressure plasma system, and (b) the temperature profile of infrared thermal imaging. Plasma conditions are 10 slm argon, 440 rpm rotational speed, and 100 watt RF plasma power.

Fig. 2. The optical emission spectrum from cyclonic atmospheric-pressure plasma. Plasma conditions are 10 slm argon and 100 watt RF plasma power.

Fig. 3. The average contact angles and the surface free energy changes of cyclonic atmospheric-pressure plasma-modified polysulfone membrane with different treatment times. Plasma conditions: argon flow rate of 10 slm and RF power input of 150 watt.

Fig. 4. The average contact angles and the surface free energy changes of cyclonic atmospheric-pressure plasma-modified polysulfone membrane with a varying argon gas flow rate. Plasma conditions: RF power input of 150 watt and treatment time of 150 sec.

Fig. 5. The average contact angles and the surface free energy changes of cyclonic atmospheric-pressure plasma-modified polysulfone membrane with a varying RF plasma power level. Plasma conditions: argon flow rate of 10 slm and treatment time of 150 sec.

Fig. 6. The average contact angles and the surface free energy changes of cyclonic atmospheric-pressure plasma-modified polysulfone membrane with distance away from downstream with argon flow rate of 10 slm, RF power input of 150 watt, Treatment time of 150 sec., Distance of 10-17.5 mm.

Fig. 7 Optical emission intensity dependence of (a) oxygen lines, (b) argon lines with distance away from downstream. Plasma conditions: argon flow rate of 10 slm, RF power input of 100 watt, Treatment time of 150sec., Distance of 0-17.5 mm.

Fig. 8. FESEM images of cyclonic atmospheric-pressure plasma–treated polysulfone membrane: (a) untreated polysulfone membrane, (b) 60 sec treatment time, (c) 150 sec treatment time.

Plasma conditions: argon flow rate of 10 slm, RF power input of 150 watt, distance of 10 mm.

Fig. 9. C 1s spectra of XPS analysis of (a) untreated polysulfone membrane and plasma–treated polysulfone membranes. Plasma conditions: RF Power : 150 Watt , 10 slm argon, and treatment time of (b) 60 sec. and (c) 150 sec.

Fig. 10. O 1s spectra of XPS analysis of (a) untreated polysulfone membrane and plasma–treated polysulfone membranes. Plasma conditions: RF Power : 150 Watt , 10 slm argon, and treatment time of (b) 60 sec. and (c) 150 sec.

Fig. 11. Size distribution of cyclonic atmospheric-pressure plasma–treated polysulfone membrane: (a) untreated polysulfone membrane, (b) 60 sec treatment time.

Table 1. Static contact angle values of two suitable liquids for the measurement of surface energy before and after plasma treatment. Plasma conditions: argon flow rate of 10 slm and RF power input of 150 watt. and treatment time of 15 sec., 30 sec., 60 sec., 90 sec., 120 sec., and 150 sec.

| Plasma treatment Time (sec)	Average contact angle (°)		Surface energy (mJ/m^2)		
	H$_2$O	Di-iodomethane	γ_s	γ_s^d	γ_s^P
0	70	29	51	45	6
15	39	35	65	42	23
30	38	34	66	42	24
60	21	36	74	42	32
90	14	37	75	41	34
120	11	37	75	41	34
150	8	36	77	41	36

Ching-Yuan Tsai, Ya-Chi Chang, and Chun Huang[*]

Table 2 Element composition/ratio (%) of C 1s and O 1s in the samples with different binding energies before and after plasma treatment. Plasma conditions: RF power input of 150 watt, argon flow rate of 10 slm, and treatment time of 60 sec. and 150 sec.

Sample	Elemental composition (%)				Elemental ratio (%)	
	C	O	N	S	O/C	S/C
Untreated PSF membrane	73.24	17.56	4.81	4.4	23.98	6.01
Ar plasma-treated at PSF membrane (60 s)	68.7	26.21	0	5.09	38.15	7.41
Ar plasma-treated at PSF membrane (150 s)	60.73	33.72	0.71	4.83	55.52	7.95

Sample	Contribution of C_{1s} components (%)					
	C-C/C-H 284.7 eV	C-S 285.3 eV	C-O 286 eV	C=O 287.1 eV	O-C=O 290.3 eV	π - π * 291.7 eV
Untreated PSF membrane	57.98	12.23	10.62	14.58	O	4.58
Ar plasma-treated at PSF membrane (60 s)	43.03	21.76	16.87	13.73	1.28	3.33
Ar plasma-treated at PSF membrane (150 s)	38.89	24.4	14.35	17.18	2.61	2.57

Sample	Contribution of O_{1s} components (%)		
	O=S=O 531.8 eV	C=O* 532.4 eV	O*-C=O 533.1 eV
Untreated PSF membrane	73.5	0	26.5
Ar plasma-treated at PSF membrane (60 s)	55	15.42	29.58
Ar plasma-treated at PSF membrane (150 s)	64.64	10.75	24.61

Ching-Yuan Tsai, Ya-Chi Chang, and Chun Huang [*]
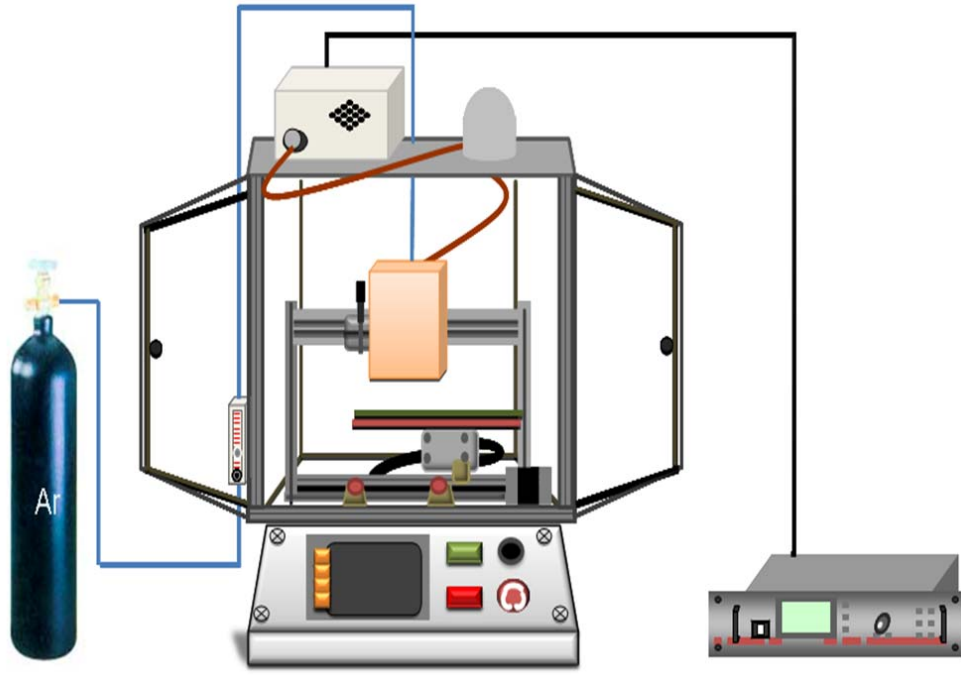
(a)
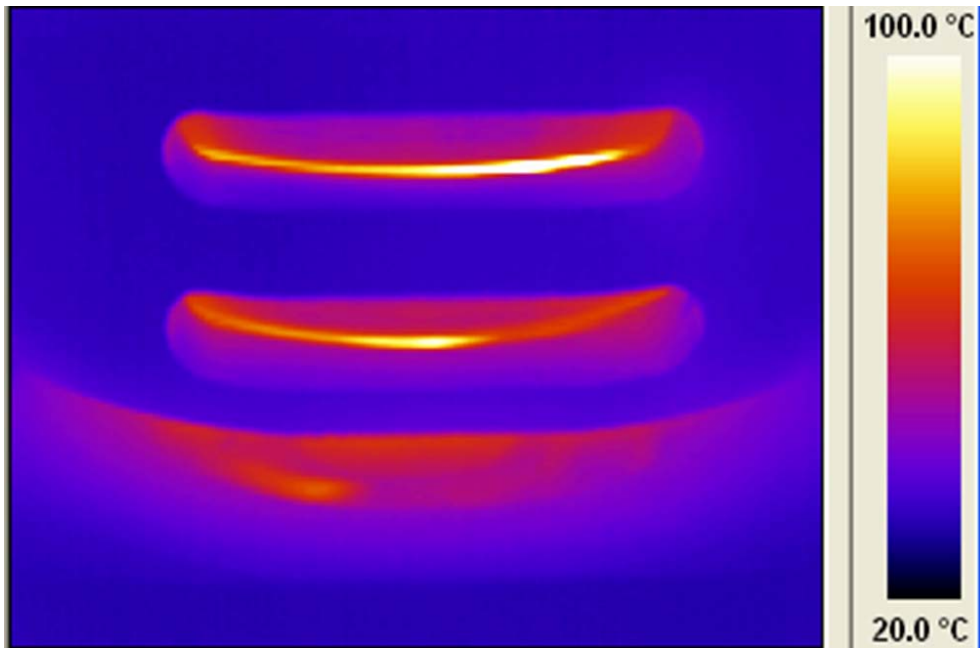
(b)

Fig. 1

Ching-Yuan Tsai, Ya-Chi Chang, and Chun Huang [*]
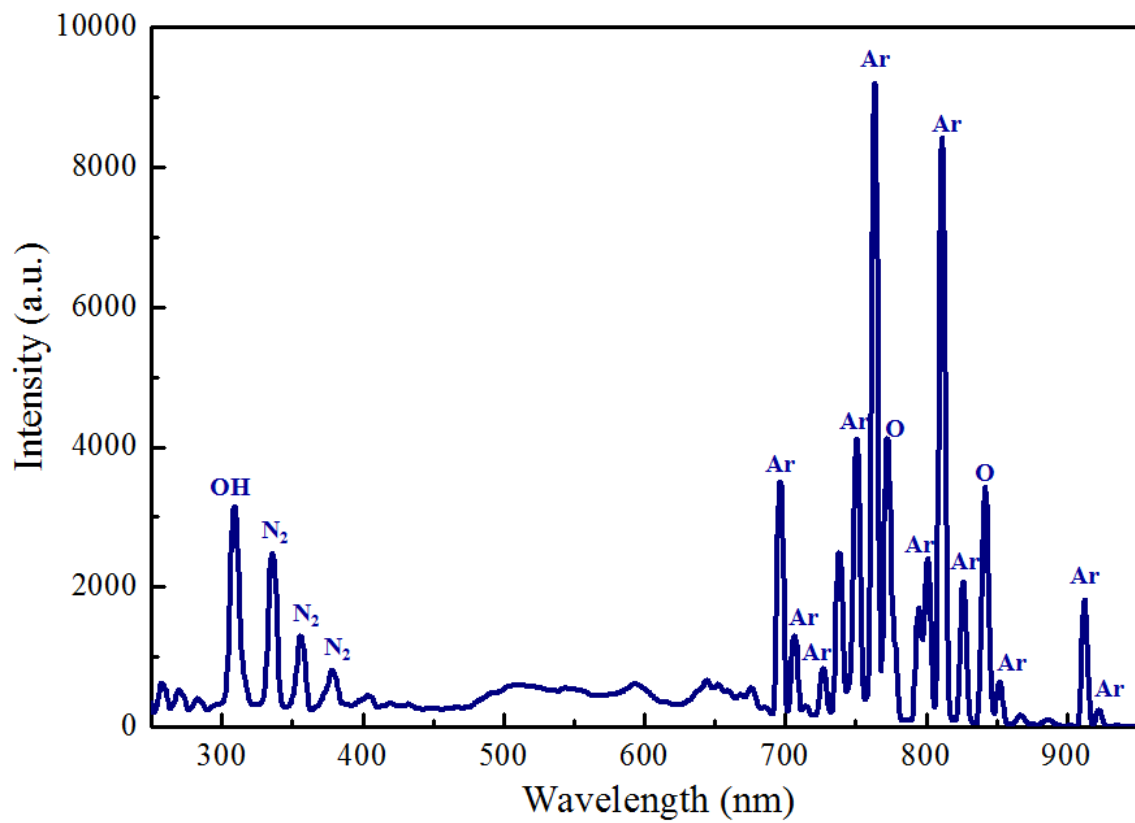
Fig. 2

Ching-Yuan Tsai, Ya-Chi Chang, and Chun Huang [*]
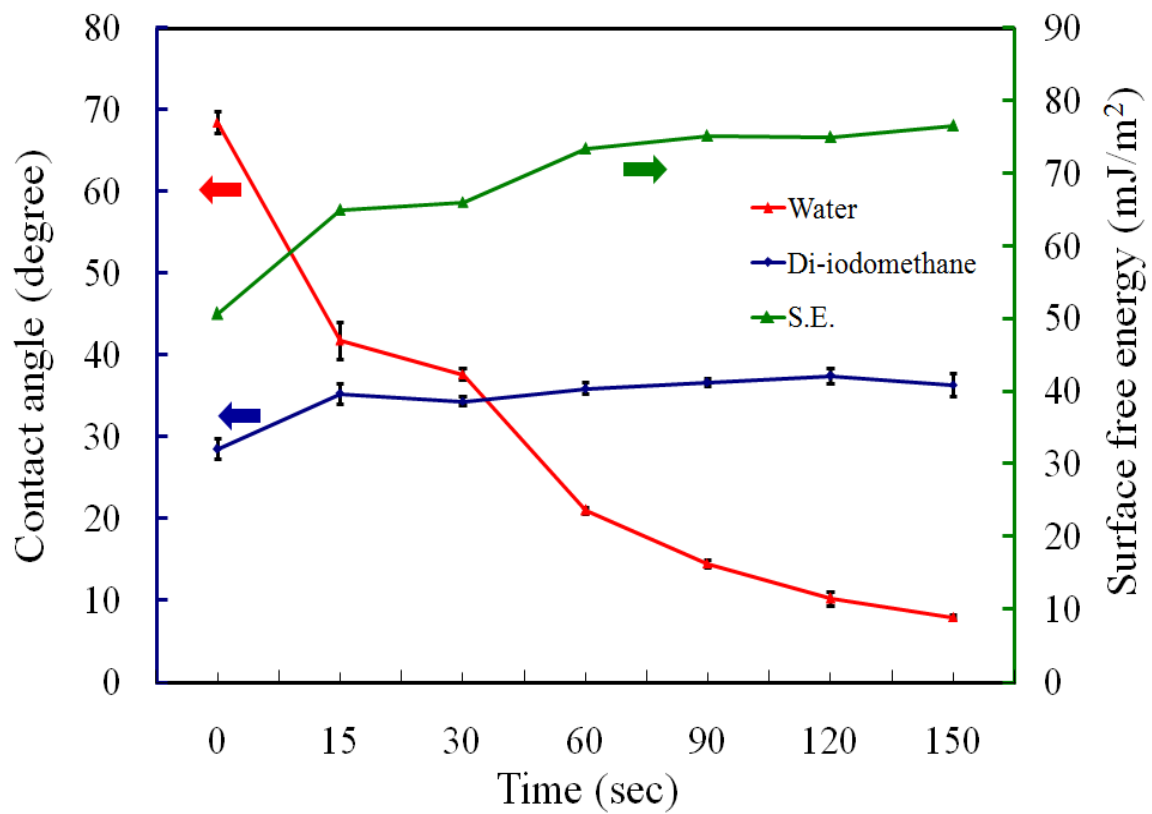
Fig. 3

Ching-Yuan Tsai, Ya-Chi Chang, and Chun Huang[*]
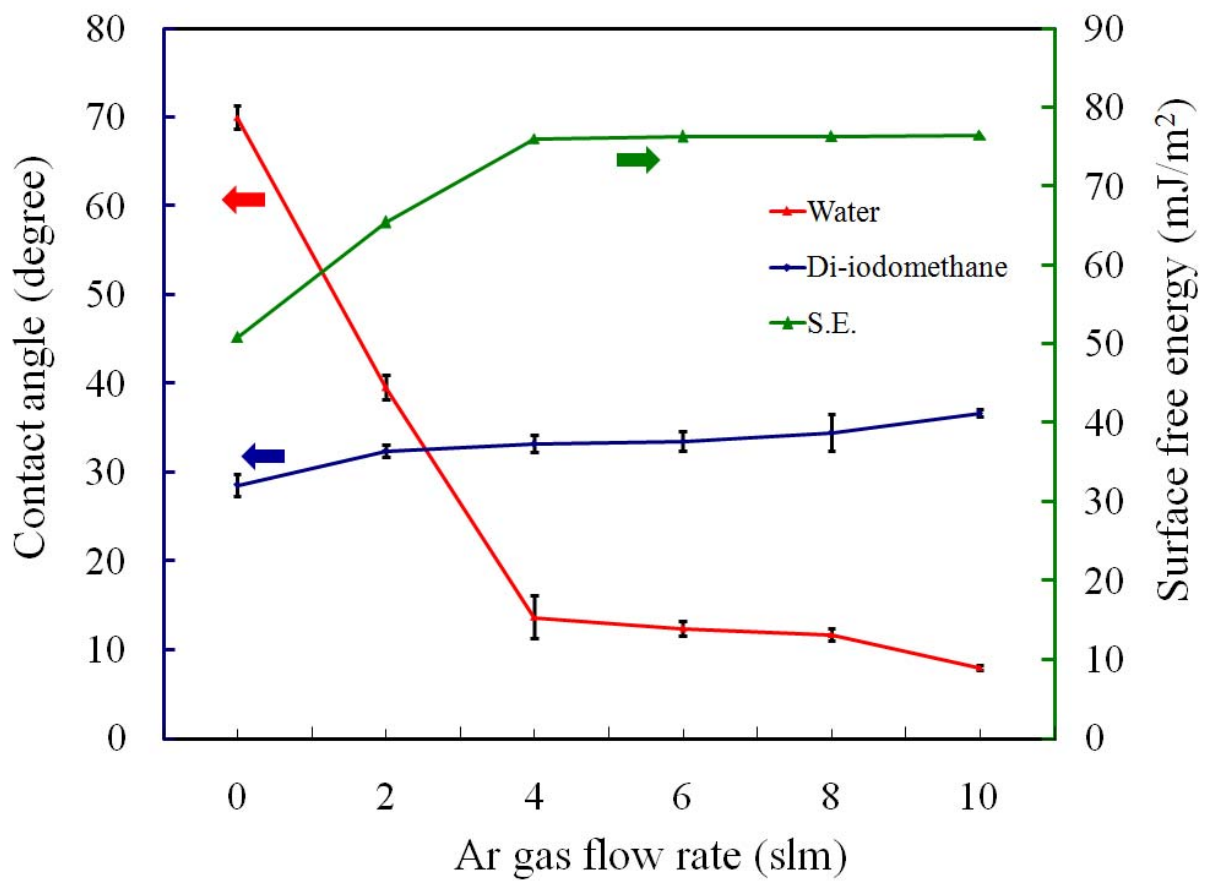
Fig. 4

Ching-Yuan Tsai, Ya-Chi Chang, and Chun Huang [*]
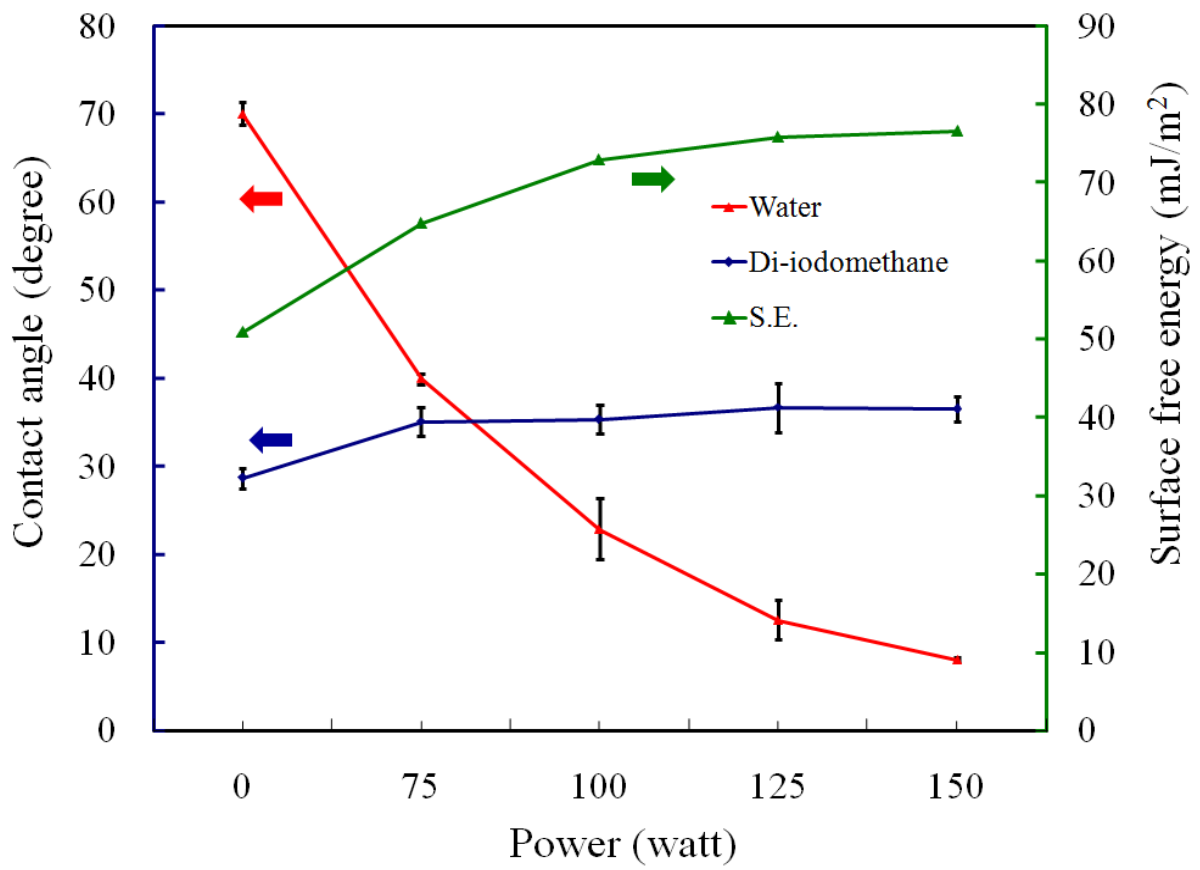
Fig. 5

Ching-Yuan Tsai, Ya-Chi Chang, and Chun Huang[*]
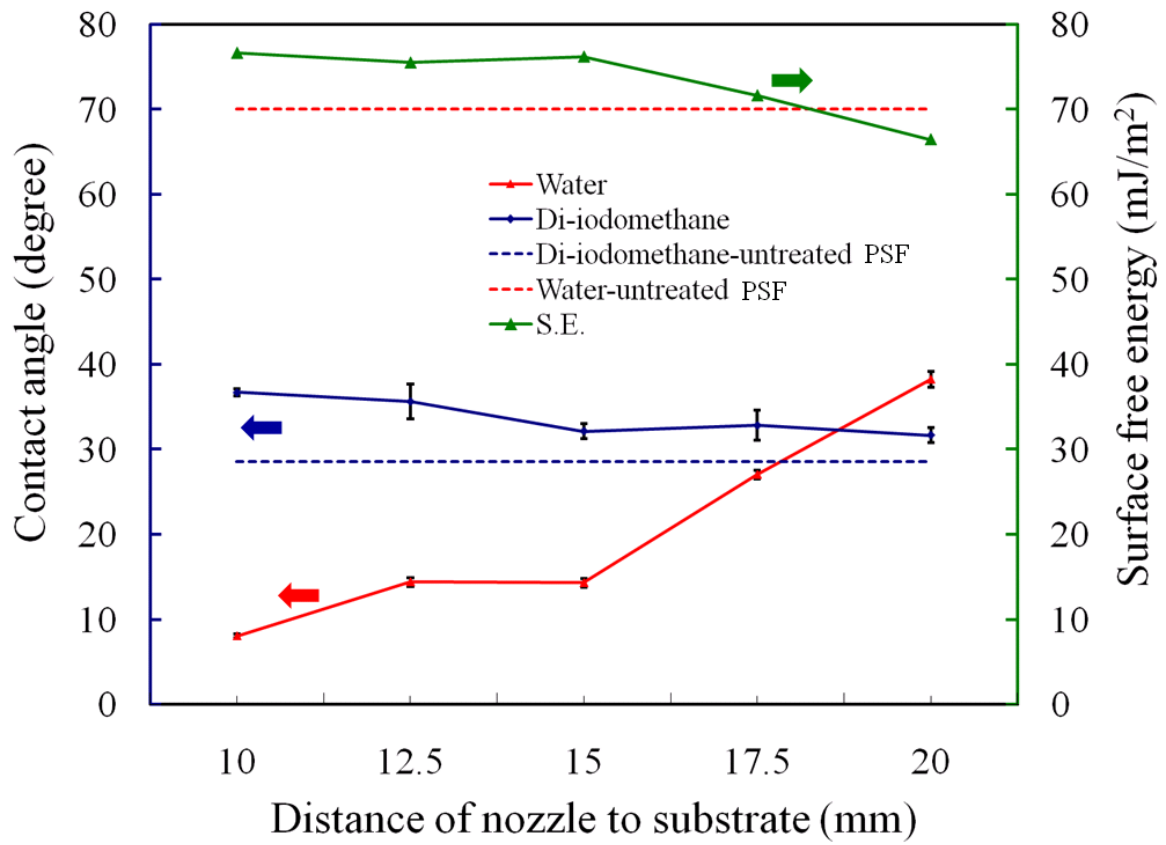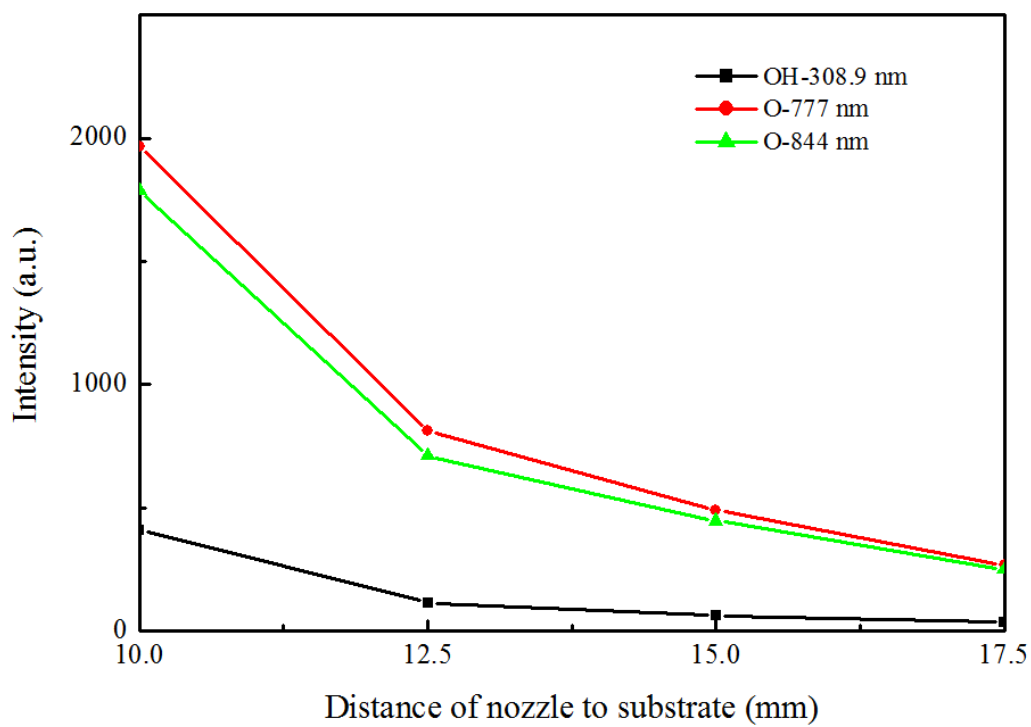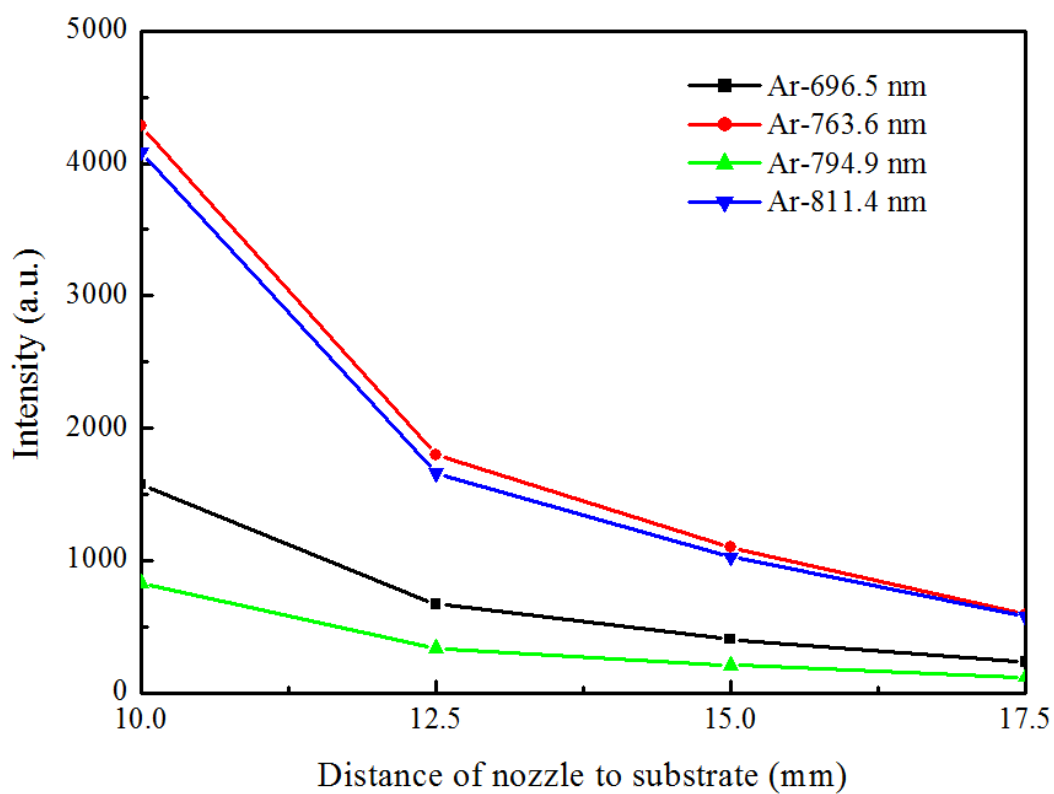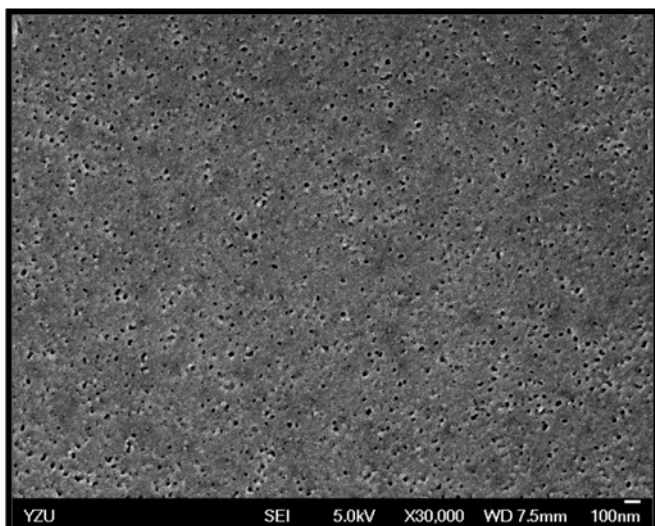
Fig. 6

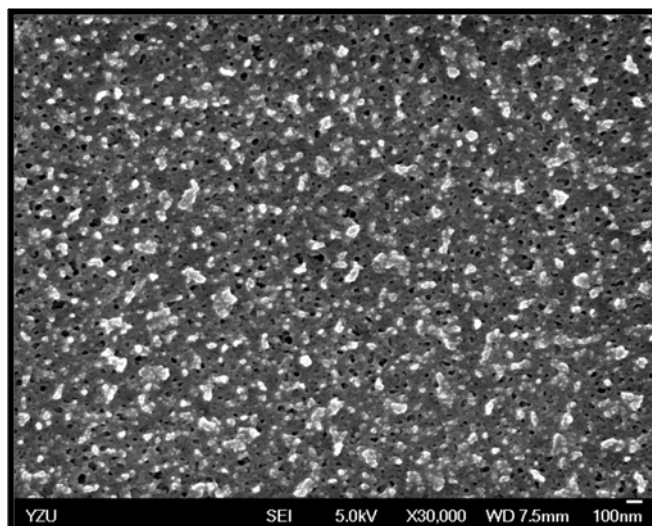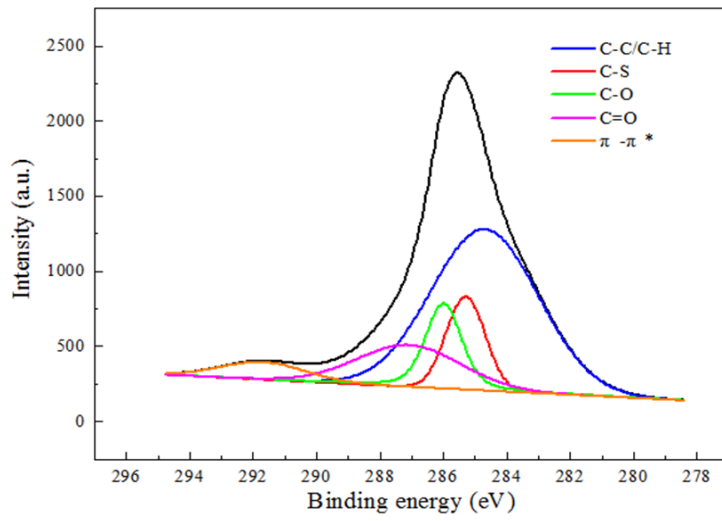Ching-Yuan Tsai, Ya-Chi Chang, and Chun Huang [*]

(a)

(b)

Fig. 7
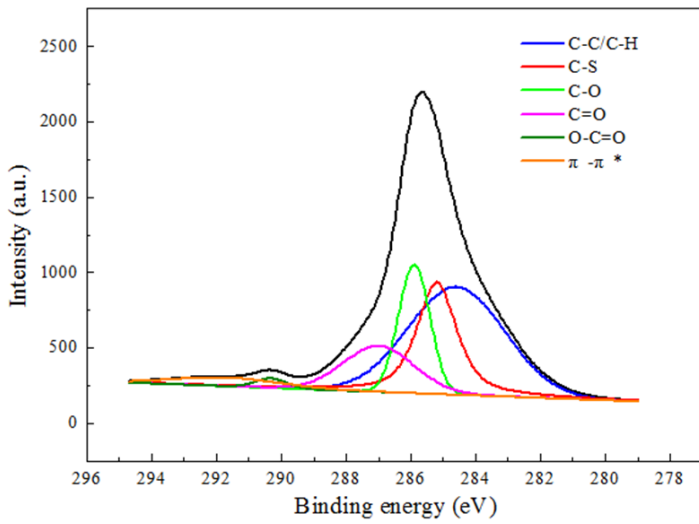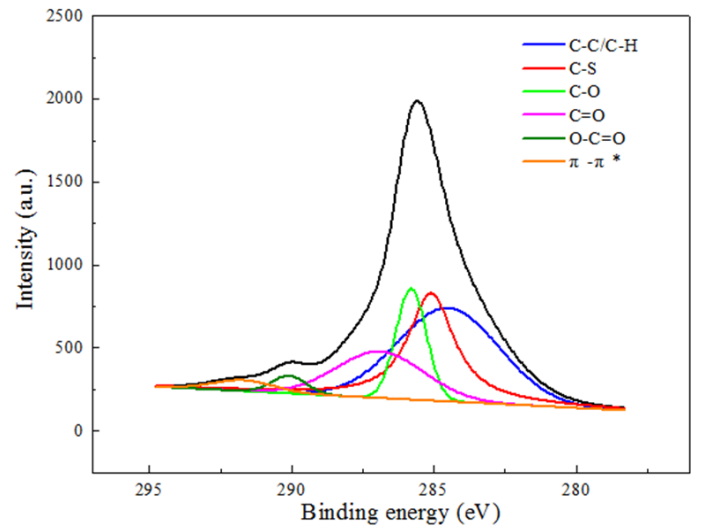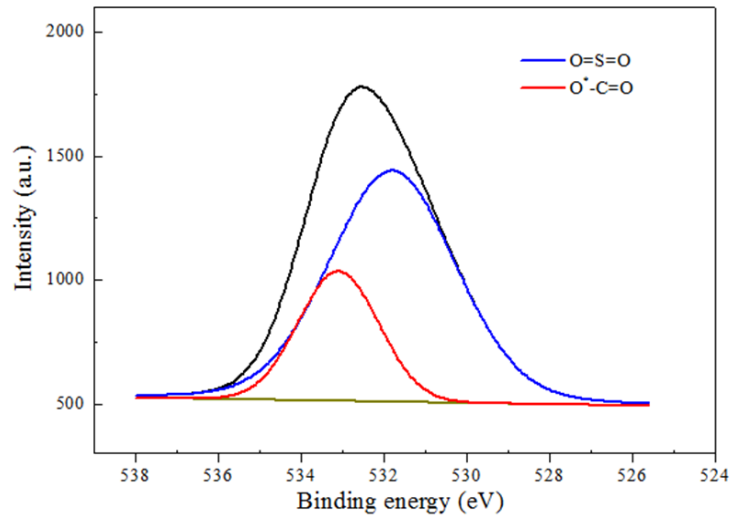
Ching-Yuan Tsai, Ya-Chi Chang, and Chun Huang[*]

(a)

(b)

(c)

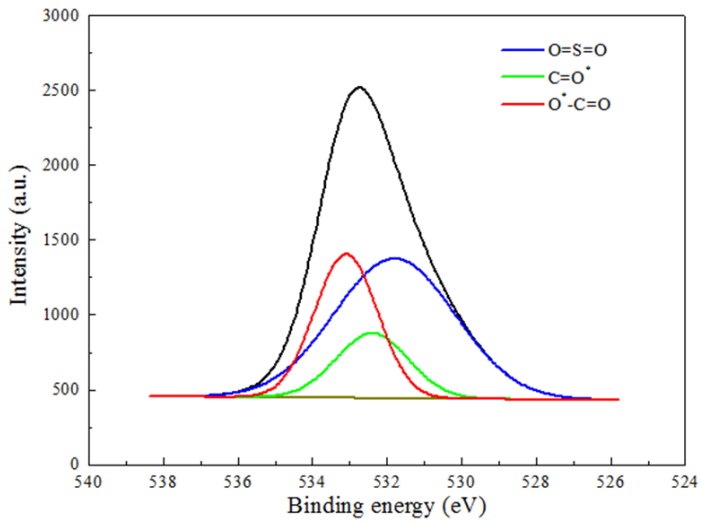Fig. 8

Ching-Yuan Tsai, Ya-Chi Chang, and Chun Huang[*]

(a)

(b)

(c)

Fig. 9
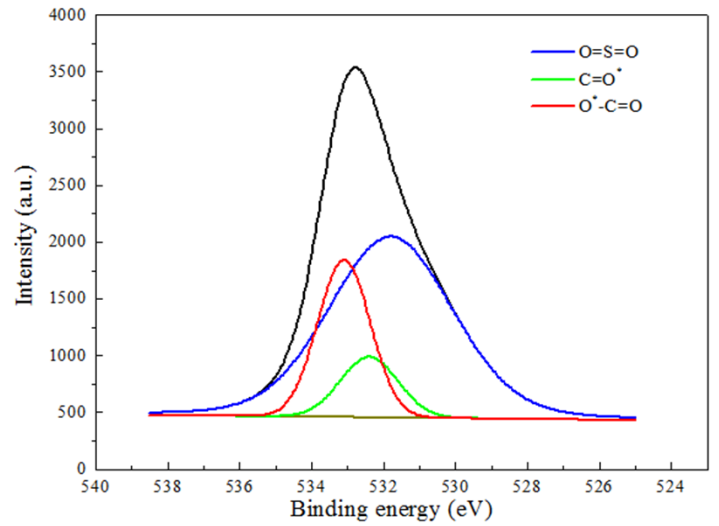
Ching-Yuan Tsai, Ya-Chi Chang, and Chun Huang[*]

25

(a)

(b)   (c)
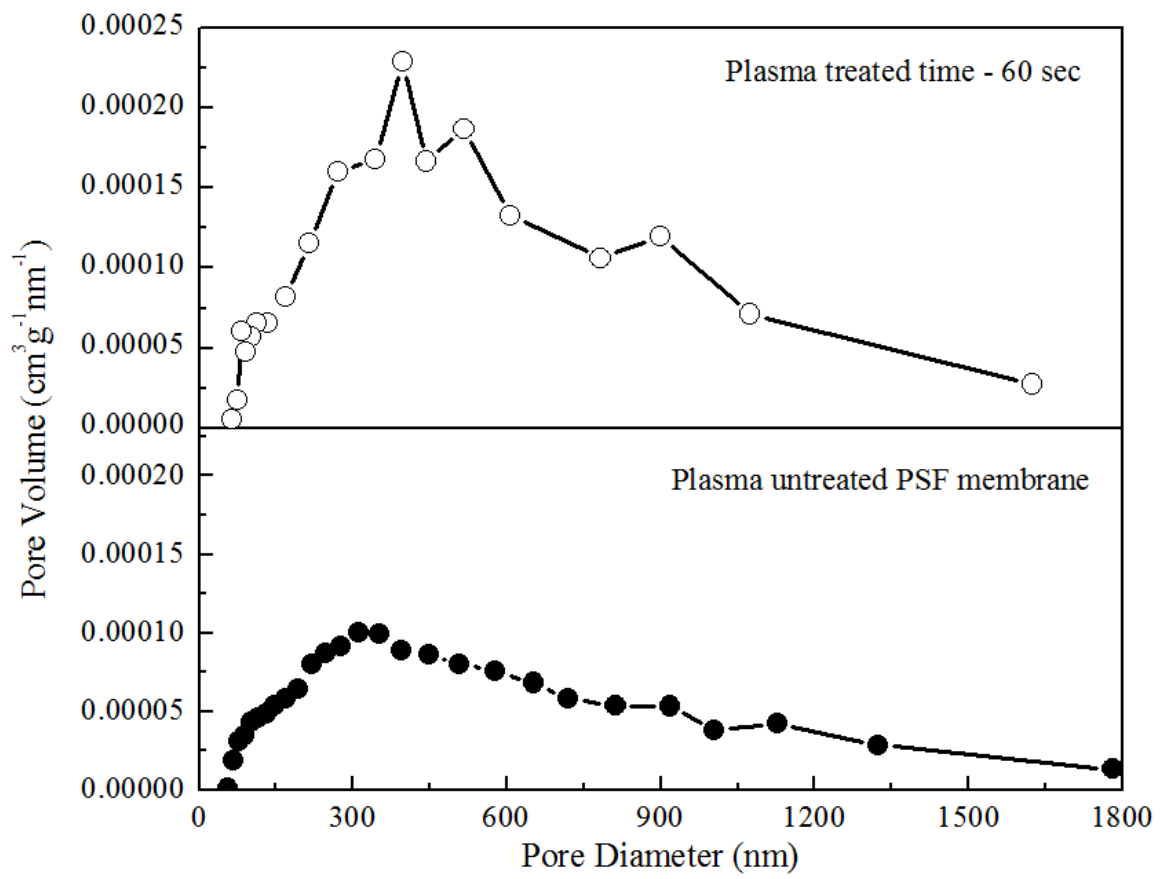
Fig. 10

Ching-Yuan Tsai, Ya-Chi Chang, and Chun Huang[*]

Fig. 11

Ching-Yuan Tsai, Ya-Chi Chang, and Chun Huang [*]